# Local Calibration of Joint Faulting Model by Using Resampling Techniques

Syed W. Haider[1], Wouter C. Brink[2], Neeraj Buch[3] and Lev Khazanovich[4]

## Abstract

The local calibration of the performance models in the Pavement-ME analysis and design procedure is a challenging task mainly because of (a) data needed to characterize the existing pavement sections, (b) nature of the performance models, and (c) inadequate number of pavement sections for a robust calibration. The transverse joint faulting model in the Pavement-ME uses a complex incremental approach. The model has eight (8) different calibration coefficients which can be adjusted to fit the measured faulting. Further, calculating predicted faulting using the published model equations is difficult. The determination of faulting outside the Pavement-ME is essential to calibrate all the model coefficients simultaneously. This paper documents the process of calculating faulting outside of the Pavement-ME by utilizing the inputs specific to the pavement sections. The first step consists of documenting the impact of each calibration coefficient on predicted faulting. This sensitivity assists in determining the most important calibration coefficient in the model. The second step is to calibrate the model by using all the available pavement sections in the calibration dataset. Multiple sampling approaches were utilized to calibrate the faulting model in the State of Michigan. First, the traditional approach uses about 70% of the data for calibration and the remaining 30% for validation. However, most of the States have a limited number of pavement sections for local calibration. Therefore, there is a need to employ statistical methodologies that are more efficient and robust for model calibrations. Second, bootstrapping and jackknifing resampling methods are used to efficiently estimate the model coefficients. The results in the paper show the effect of different sampling approaches on model parameter estimations and compare the role of such parameters in reducing the bias and the standard error of the faulting model.

## Background

The rigid pavement performance prediction models in the Pavement-ME predict transverse cracking, transverse joint faulting and IRI. This paper focusses on the local calibration of the faulting model that predicts the mean transverse joint faulting on a monthly basis using an incremental approach. The faulting accumulates over the design

[1] Associate Professor, Department of Civil and Environmental Engineering, Michigan State University, 3546 Engineering Building, East Lansing, MI-48824; PH (517) 353-9782; FAX (517) 432-1827; email: syedwaqa@egr.msu.edu

[2] Staff Civil Engineer , Applied Research Associates, 100 Trade Centre Dr., Suite 200, Champaign, IL-61820; email: wbrink@ara.com

[3] Professor, Department of Civil and Environmental Engineering, Michigan State University, 3546 Engineering Building, East Lansing, MI-48824

[4] Professor, Department of Civil, Environmental, and Geo- Engineering, University of Minnesota, 160 Civil Engineering Building, Minneapolis, MN-55455; email: khaza001@umn.edu

life of the pavement. The local calibration of the faulting model consists of adjusting the calibration coefficients to minimize the error and bias between the measured and predicted faulting. Several State Highway Agencies (SHAs) have performed local calibration of the transverse joint faulting model. The calibration coefficients obtained from various SHA's and national calibrations are summarized in Table 1 (Fick 2010; Haider et al. 2014; Mallela et al. 2015; Pierce and McGovern 2014).

Table 1 Faulting Model Local Calibration Coefficients

| Calib. Coeff. | National | AZ | CO | FL | WA un-doweled | WA DBR | Revised National | MI |
|---|---|---|---|---|---|---|---|---|
| C1 | 1.0184 | 0.0355 | 0.5104 | 4.0472 | 0.4 | 0.934 | 0.5104 | 0.4 |
| C2 | 0.91656 | 0.1147 | 0.00838 | 0.91656 | 0.341 | 0.6 | 0.00838 | 0.91656 |
| C3 | 0.002848 | 0.00436 | 0.00147 | 0.002848 | 0.000535 | 0.001725 | 0.00147 | 0.002848 |
| C4 | 0.00088 | 1.1E-7 | 0.008345 | 0.00088 | 0.000248 | 0.004 | 0.00834 | 0.00088 |
| C5 | 250 | 20000 | 5999 | 250 | 77.5 | 250 | 5999 | 250 |
| C6 | 0.4 | 2.309 | 0.8404 | 0.0790 | 0.0064 | 0.4 | 0.8404 | 0.4 |
| C7 | 1.8331 | 0.189 | 5.9293 | 1.8331 | 2.04 | 0.65 | 5.9293 | 1.8331 |
| C8 | 400 | 400 | 400 | 400 | 400 | 400 | 400 | 400 |

### Transverse Joint Faulting Model

The mean transverse joint faulting is predicted on a monthly basis using an incremental approach. A faulting increment is determined each month and the current faulting level affects the magnitude of the increment. The monthly prediction of faulting essentially takes into account the seasonal variations within a year. The faulting at each month is determined as a sum of faulting increments from all previous months in the pavement life from the traffic opening date using the following equations:

$$Fault_m = \sum_{i=1}^{m} \Delta Fault_i \tag{1}$$

$$\Delta Fault_i = C_{34} \times (FAULTMAX_{i-1} - Fault_{i-1})^2 \times DE_i \tag{2}$$

$$FAULTMAX_i = FAULTMAX_0 + \mathrm{C}_7 \times \frac{\sum_{j=1}^{m} DE_j}{216000} \times Log(1 + \mathrm{C}_5 \times 5.0^{EROD})^{C_6} \tag{3}$$

$$FAULTMAX_0 = \mathrm{C}_{12} \times \delta_{\mathrm{curling}} \times \left[ Log(1 + C_5 \times 5.0^{EROD}) \times Log(\frac{P_{200} \times WetDays}{p_s}) \right]^{C_6} \tag{4}$$

where:

| | | |
|---|---|---|
| $Fault_m$ | = | Mean joint faulting at the end of month *m*, in. |
| $\Delta Fault_i$ | = | Incremental change (monthly) in mean transverse joint faulting during month *i*, in. |
| $FAULTMAX_i$ | = | Maximum mean transverse joint faulting for month *i*, in. |
| $FAULTMAX_0$ | = | Initial maximum mean transverse joint faulting, in. |
| $EROD$ | = | Base/sub-base erodibility factor |
| $DE_i$ | = | Differential density of energy for subgrade deformation accumulated during month *i* |
| $\delta_{curling}$ | = | Maximum mean monthly slab corner upward deflection due to temperature curling and moisture warping. |
| $P_S$ | = | Overburden on subgrade, lb. |
| $P_{200}$ | = | Percent subgrade material passing #200 sieve. |
| $WetDays$ | = | Average annual number of wet days (greater than 0.1 inch rainfall). |

| | | |
|---|---|---|
| $C_{1,2,3,4,5,6,7,12,34}$ | = | Global calibration constants ($C_1$ = 1.0184; $C_2$ = 0.91656; $C_3$ = 0.002848; $C_4$ = 0.0008837; $C_5$ = 250; $C_6$ = 0.4; $C_7$ = 1.8331) |

$$C_{12} = C_1 + C_2 \times FR^{0.25} \tag{5}$$

$$C_{34} = C_3 + C_4 \times FR^{0.25} \tag{6}$$

where:

| | | |
|---|---|---|
| $FR$ | = | Base freezing index defined as percentage of time the top base temperature is below freezing (32 °F) temperature. |

Since the calculating mean joint faulting from the above equations is an iterative procedure and not very intuitive, the following section describes the faulting calculation outside the Pavement-ME software.

### Calculating Faulting Outside the Pavement-ME Software

In order to calibrate all the coefficients simultaneously, the predicted faulting needs to be calculated outside the Pavement-ME software using the faulting model equations presented above. The predicted faulting is dependent on many input variables. These input variables are used to calculate the initial maximum faulting and the subsequent monthly faulting. The monthly faulting calculations accumulate over the pavement design life. Figure 1 shows the incremental approach to calculate faulting from the intermediate output files.

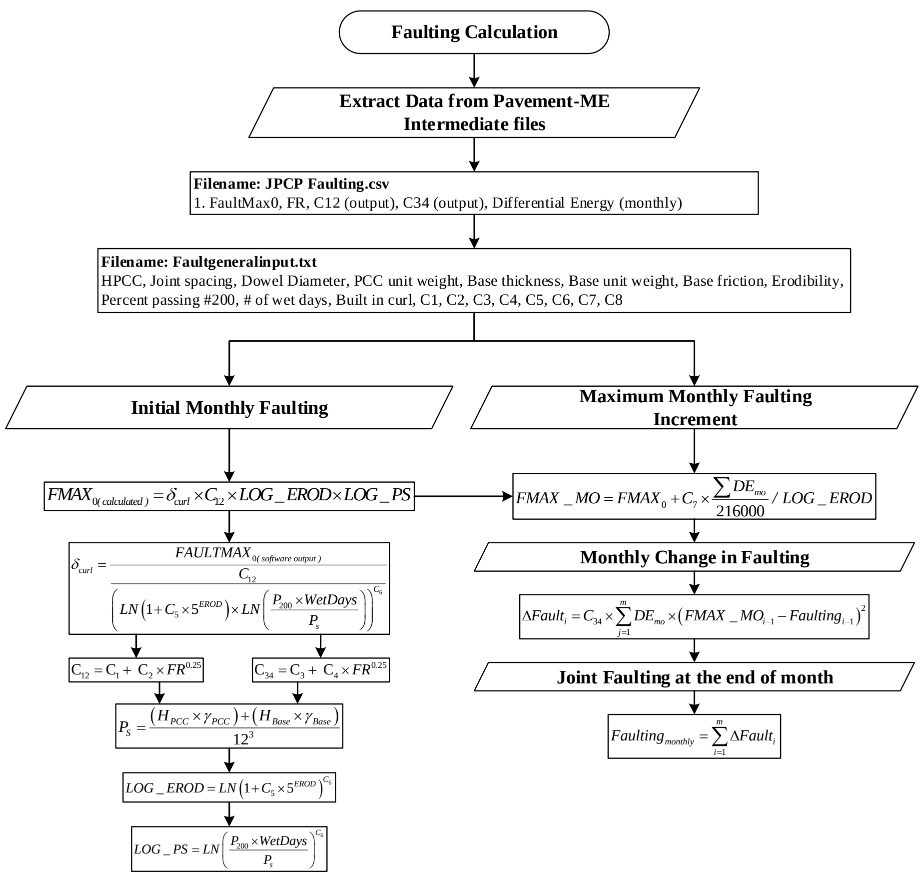


Figure 1 Mean joint faulting calculation procedure

The faulting model has eight different calibration coefficients. These calibration coefficients affect many different aspects of the model. It should be noted that some of the faulting model equations are different than previously presented in the MEPDG Manual of Practice (AASHTO 2008). Therefore, this section outlines the process for calculating the mean transverse joint faulting using inputs from the Pavement-ME. The first step consists of extracting the necessary inputs from the Pavement-ME intermediate files. The "FaultMax$_0$", "FR", C12, C34, and differential energy are extracted from the "JPCP_faulting.csv" file located in the intermediate files. Figure 2 shows the location of the four different inputs.

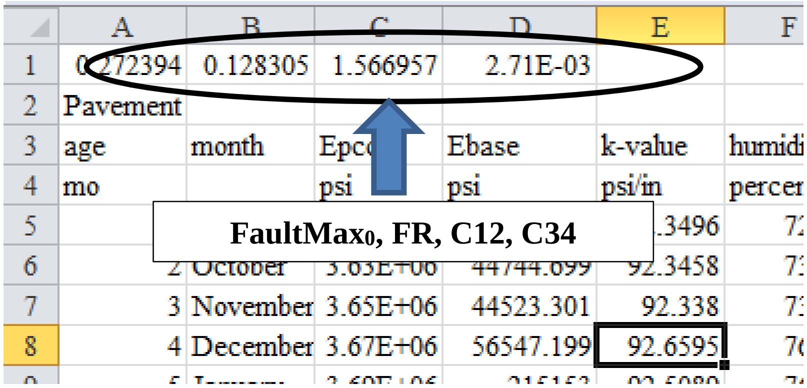


Figure 2 Input required for faulting calculations from JPCP_faulting.csv file

The general faulting inputs are extracted from the "faultgeneralinput.txt" file and are listed below:

- PCC thickness
- Joint Spacing
- Dowel Diameter
- PCC unit weight
- Base thickness
- Base unit weight
- Base friction
- Erodibility
- Percent passing sieve #200
- # of wet days
- Built in curl
- C1, C2, C3,C4, C5, C6, C7, C8

Figure 3 shows details of inputs in the faultgeneralinput.txt file. These input values are used to calculate monthly faulting over the pavement design life. The updated faulting model equations are presented below. The overburden pressure above the subgrade is calculated by Equation(7).

$$P_S = \frac{(H_{PCC} \times \gamma_{PCC}) + (H_{Base} \times \gamma_{Base})}{12^3} \tag{7}$$

where:

$P_s$ = Overburden pressure on Subgrade
$H_{PCC}$ = PCC thickness (in.)
$\gamma_{PCC}$ = PCC unit weight (lb/ft$^3$)
$H_{Base}$ = Base thickness
$\gamma_{Base}$ = Base unit weight (lb/ft$^3$)

The deflection due to slab curling ($\delta_{curl}$) is calculated internally. Equation (8) can be used to determine the $FAULTMAX_0$ (initial faulting maximum value).

$$\delta_{curl} = \frac{\dfrac{FAULTMAX_{0(\,software\ output\,)}}{C_{12}}}{\left(LN\left(1+C_5\times 5^{EROD}\right)\times LN\left(\dfrac{P_{200}\times WetDays}{P_s}\right)\right)^{C_6}} \tag{8}$$

where:

| | | |
|---|---|---|
| $\delta_{curl}$ | = | Maximum mean monthly slab corner upward deflection due to temperature curling and moisture warping. |
| $FAULTMAX_0$ | = | Initial Maximum Faulting (in.) |
| $C_{12}$ | = | Calibration coefficient: $C_{12} = C_1 + C_2 \times FR^{0.25}$, FR = Freezing Index |
| $C_5$ | = | Calibration coefficient |
| $EROD$ | = | Erodibility factor |
| $P_{200}$ | = | Percent subgrade material passing #200 sieve. |
| $WetDays$ | = | Average annual number of wet days (greater than 0.1 inch rainfall). |
| $Ps$ | = | Overburden pressure on subgrade |

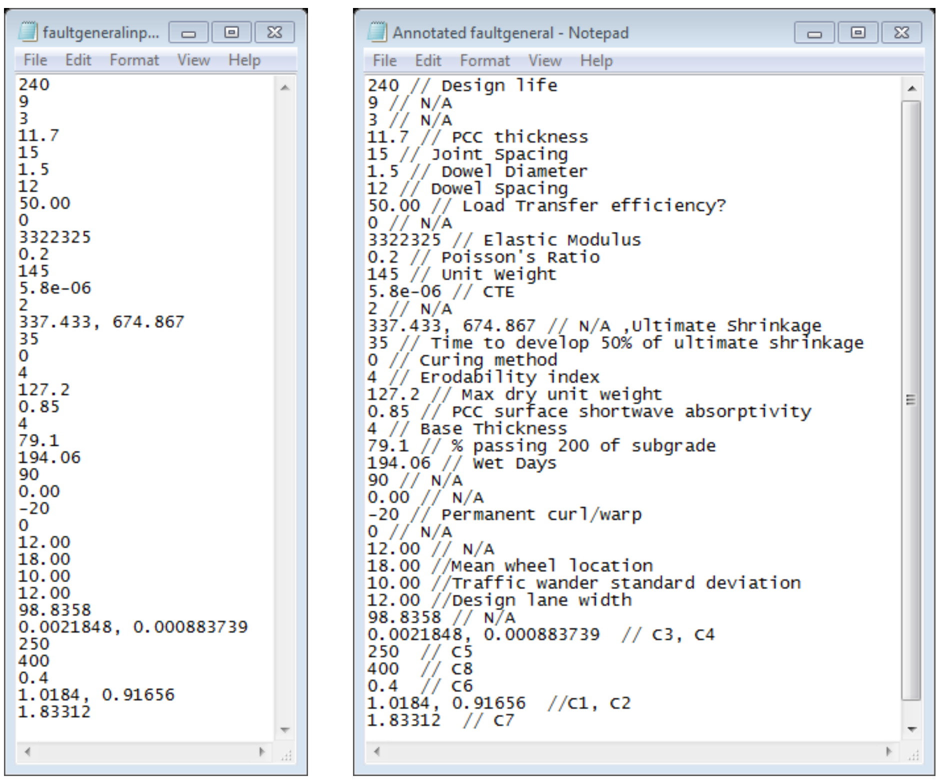


(a) Original faultgeneral.txt file (b) Annotated faultgeneral.txt file

Figure 3 General inputs for the faulting model

Further, initial maximum faulting value can be calculated by using Equations (9) through (13):

$$FMAX_{0(\,calculated\,)} = \delta_{curl} \times C_{12} \times LOG\_EROD \times LOG\_PS \tag{9}$$

$$LOG\_EROD = LN\left(1 + C_5 \times 5^{EROD}\right)^{C_6} \tag{10}$$

$$LOG\_PS = LN\left(\frac{P_{200} \times WetDays}{P_s}\right)^{C_6} \tag{11}$$

$$\mathrm{C}_{12} = \mathrm{C}_1 + \mathrm{C}_2 \times FR^{0.25} \tag{12}$$

$$\mathrm{C}_{34} = \mathrm{C}_3 + \mathrm{C}_4 \times FR^{0.25} \tag{13}$$

The monthly faulting increment is calculated by using Equation (14):

$$FMAX\_MO_i = FMAX_0 + \frac{C_7 \times \left(\frac{DE_{mo}}{216000}\right)}{LOG\_EROD} \tag{14}$$

where:

| | | |
|---|---|---|
| $FMAX\_MO_i$ | = | Maximum mean transverse joint faulting for month *i*, (in.) |
| $FMAX_0$ | = | Initial maximum mean transverse joint faulting (in.) |
| $DE_{mo}$ | = | Differential Energy accumulated during month (i) |
| $LOG\_EROD$ | = | Erodibility defined in Equation (10) |

The monthly increment and cumulative faulting values are determined by using Equations (15) and (16), respectively:

$$\Delta Fault_i = C_{34} \times \sum_{j=1}^{m} DE_{mo} \times \left(FMAX\_MO_{i-1} - Faulting_{i-1}\right)^2 \tag{15}$$

$$Faulting_{monthly} = \sum_{i=1}^{m} \Delta Fault_i \tag{16}$$

where:

| | | |
|---|---|---|
| $Faulting_{monthly}$ | = | Mean joint faulting at the end of month *m*, in. |
| $\Delta Fault_i$ | = | Incremental change (monthly) in mean transverse joint faulting during month *i*, in. |
| $FMAX\_MO_i$ | = | Maximum mean transverse joint faulting for month *i*, in. |

The faulting predictions from the Pavement-ME software can be replicated using Equations (7) through(16). This method was tested for several pavement sections and the results had a perfect match between the Pavement-ME outputs and calculated faulting values.

**Sensitivity of Faulting Model Calibration Coefficients**

The faulting value calculations outside the software are essential in the local calibration process of the faulting model. The calculated faulting values are used to calibrate all the model coefficients simultaneously using optimization tools and the calibration process do not require to rerun the software every time a coefficient is changed. Consequently, this method will significantly reduce the time needed for local calibration. Figure 4 shows the sensitivity of all the faulting model calibration coefficients. The impact of the $C_1$ and $C_2$ calibration coefficients are shown in Figures 4a and 4b. These coefficients directly affect the overall magnitude of predicted transverse joint faulting. The $C_3$ and $C_4$ calibration coefficients affect the early age faulting predictions as observed in Figures 4c and 4d.

The $C_5$ and $C_6$ coefficients seem to have insignificant impact on the predicted faulting as shown in Figures 4e and 4f. These coefficients are related to the erodibility factor for a particular pavement section. The impacts may not be apparent because all factors are held constant in this case. The $C_7$ calibration coefficient affects the slope of faulting predictions at later stages of pavement life as shown in Figure 4g.

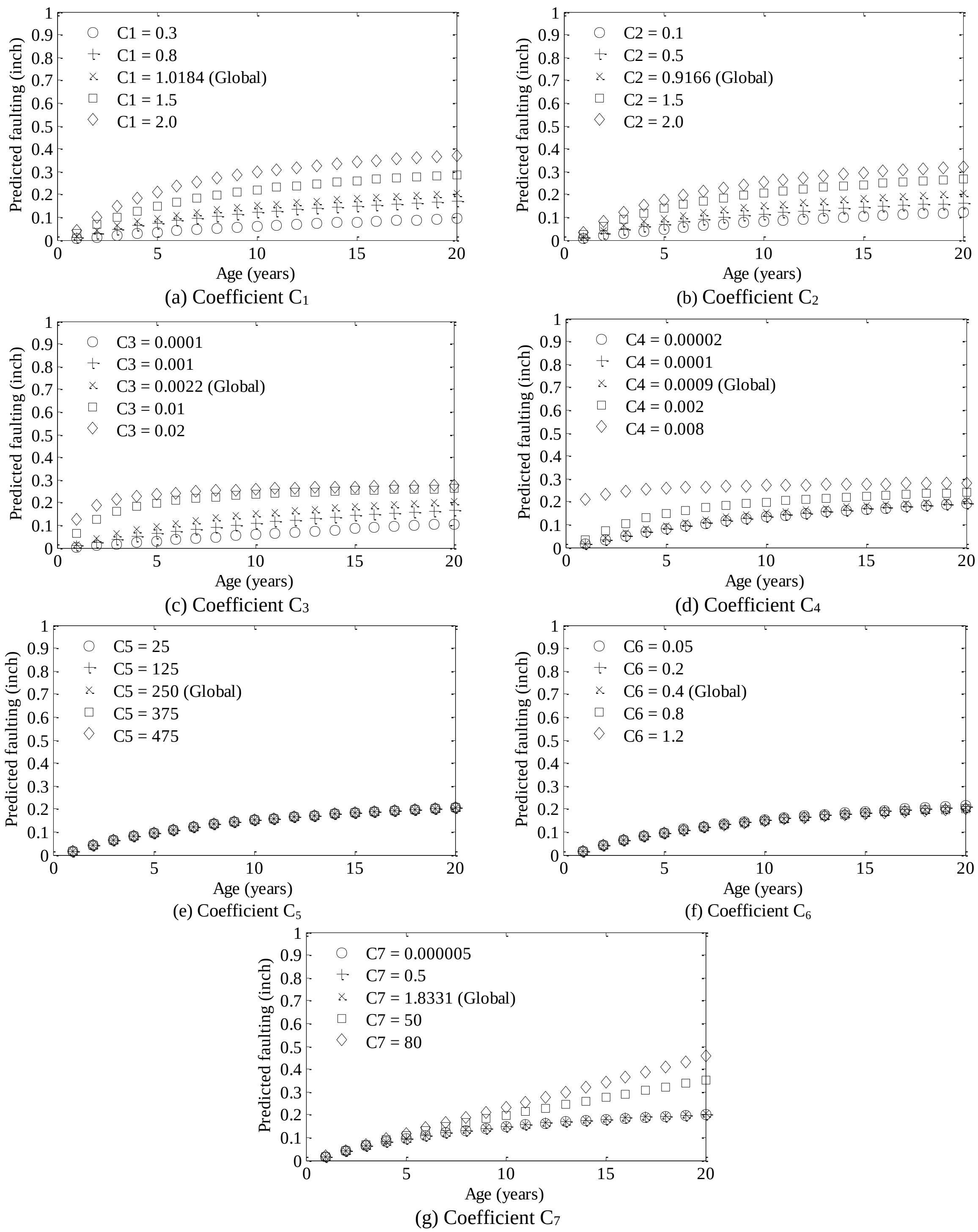


(a) Coefficient $C_1$

(b) Coefficient $C_2$

(c) Coefficient $C_3$

(d) Coefficient $C_4$

(e) Coefficient $C_5$

(f) Coefficient $C_6$

(g) Coefficient $C_7$

Figure 4 Sensitivity of the faulting model calibration coefficients

## Local Calibration of the Faulting Model

The faulting model calibration requires varying seven calibration coefficients simultaneously in order to minimize the sum of squared error (SSE) between the measured and predicted faulting. The initial faulting model local calibration in the State of Michigan only adjusted the $C_1$ coefficient since this has significant impact on the predicted faulting. In addition, the reason for only changing $C_1$ was that the predicted faulting from the Pavement-ME could not be replicated outside of the software. Subsequently, additional efforts were made to evaluate the faulting model predictions outside the Pavement-ME software. This section describes the methods adopted to locally calibrate the faulting model coefficients simultaneously using measured faulting values in the State of Michigan.

Three calibration sampling methods were used to compare the calibration coefficients, model standard error and bias. These methods include:

- No sampling (use the entire dataset)
- Split sampling (70% for calibration 30% for validation)
- Bootstrapping validation (80% for calibration, 20% for validation)

Several methods can be used to adjust the local calibration coefficients of the faulting model. The first and most inefficient method consists of changing the calibration coefficients in the Pavement-ME software and running it every time. This method does not provide the best estimate of the calibration coefficients because the ranges of coefficients may not be fine enough for a particular calibration coefficient and the interactive effects may not be captured. The second method consists of coding the faulting prediction equations outside of the Pavement-ME and using statistical software such as SAS or MS Excel Solver to numerically optimize the model by changing the calibration coefficients. Such calibration was performed when the global model's calibration coefficients were updated to consider the modified measurements of the coefficient of thermal expansion (CTE)(Mallela et al. 2015; Sachs et al. 2015). The third method consists of using the genetic algorithm (GA) optimization technique available in the MATLAB Software (MathWorks 2015). In general, the GA can solve constrained and unconstrained optimization problems based on processes from biological evolution. The GA was used for the faulting model calibration to modify the solutions in a population (calibration coefficients). The individual values within a population are randomly selected to represent parent functions which are then used to determine the children for the next generation. This process is repeated and the population eventually reaches an optimal solution (MathWorks 2015). One benefit of the GA is that it is capable of converging to a unique global minimum regardless of if any local minima exist (Varma et al. 2013). The GA-based optimization was performed by using the MATLAB "*ga"* function. The optimization function consisted of minimizing the SSE between the predicted and measured faulting as shown in Equation(17).

$$Error = \sum \left( Faulting_{Predicted} - Faulting_{Measured} \right)^2 \qquad (17)$$

The error was minimized by varying the seven calibration coefficients in the faulting model. The calibration coefficients were constrained to ensure reasonable results. The lower and upper bound constraints were set based on the global model calibration coefficient values to ensure a broad range for each population in the GA. The constraints used for each calibration coefficient are summarized in Table 2.

Table 2 Faulting model calibration coefficient constraints

| Calibration coefficient | Global | Lower bound | Upper bound |
|---|---|---|---|
| C1 | 1.0184 | 0.1 | 1.32392 |
| C2 | 0.9166 | 0.4583 | 1.19158 |
| C3 | 0.0022 | 0.00286 | 0.0066 |
| C4 | 0.0009 | 0.00045 | 0.0027 |
| C5 | 250 | 125 | 5000 |
| C6 | 0.4 | 0.2 | 0.52 |
| C7 | 1.8331 | 0.91655 | 2.38303 |

The GA was executed by selecting 300 random samples for each calibration coefficient between the lower and upper bounds specified in Table 2. This population produces a 300×7 matrix of possible combinations to search for an optimal solution. Once an optimum solution is found for a particular population, these values are used to generate another matrix and the process is repeated (generations). Thirty generations were used for the faulting model local calibration. This method would be computationally impossible if it was performed manually by changing each calibration coefficient and running the Pavement-ME.

The results for the no sampling split sampling and bootstrapping validation techniques are summarized below. Figures 5 and 6 summarize the standard error of estimate (SEE) and bias for the various sampling techniques. The results show that the SSE and bias was reduced after local calibration for all sampling methods when compared with the global faulting model. All sampling methods showed somewhat similar magnitudes for SEE and bias. However, the SEE and bias for bootstrap validation method is much lower as compared to others, especially for the model validation.

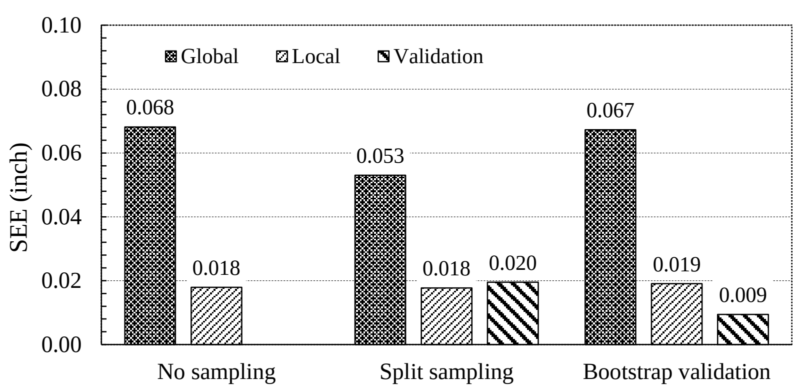


Figure 5 Summary of standard error for all sampling techniques

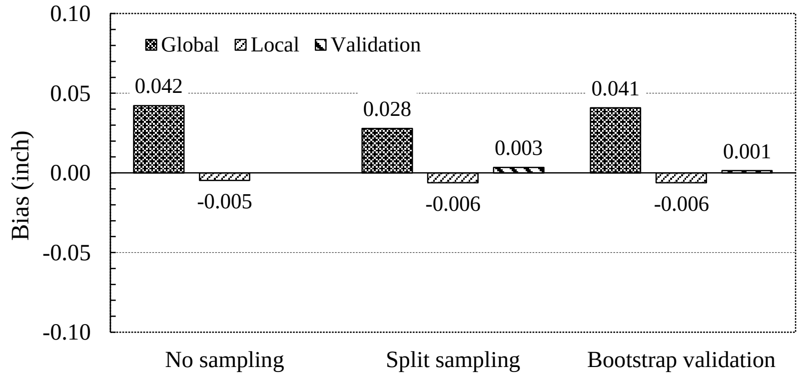


Figure 6 Summary of bias for all sampling techniques

The faulting model calibration coefficients for all sampling methods are summarized in Table 3. It can be seen from the results that the coefficients were similar between the no sampling and split sampling options with slight variations. The bootstrapping validation option showed a larger difference compared to the other two sampling techniques. These results are expected because the bootstrapping validation takes into account the average of 1000 bootstrap samples and can capture the overall variability in the dataset. Figure 7 shows the distribution of the standard error and bias for the 1000 bootstraps. The mean, median and confidence intervals are also shown in the figure.

Table 3 Faulting model calibration coefficients

| Sampling Technique | Global Model | No sampling | Split sampling | Bootstrap validation |
|---|---|---|---|---|
| C1 | 1.0184 | 0.10417 | 0.10417 | 0.13188 |
| C2 | 0.9166 | 0.46669 | 0.51552 | 0.48129 |
| C3 | 0.0022 | 0.00653 | 0.00657 | 0.00524 |
| C4 | 0.0009 | 0.00255 | 0.00265 | 0.00247 |
| C5 | 250 | 4940.03 | 4887.16 | 4600.59 |
| C6 | 0.4 | 0.48839 | 0.51088 | 0.50979 |
| C7 | 1.8331 | 0.92048 | 0.95148 | 0.95246 |

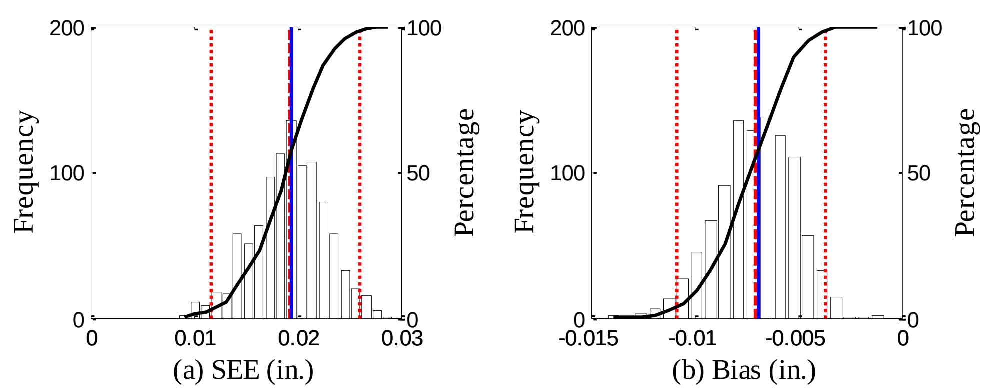


Figure 7 Frequency distributions of SEE and bias—bootstrapping validation

Hypothesis testing was performed to determine if there was a significant difference between the measured and predicted faulting. Table 4 shows the results of hypothesis tests. Significant differences between the measured and predicted faulting were observed even after local calibration. However, for the split sampling and bootstrapping techniques, the validation sections had a *p*-value greater than 0.05 which indicates that there is no significant difference between the measured and predicted faulting for the pavement sections not included in the local calibration. Figure 8 shows the comparison between the measured and predicted faulting before and after local calibration. The global model coefficients were used for the validation sections in Figure 8(a) to compare the faulting predictions before and after local calibration. The global faulting model over-predicts measured faulting for Michigan pavement sections. The locally calibrated model improves the faulting predictions significantly.

Table 4 Hypothesis testing *p*-value results

| Sampling Technique | Global | Local | Validation |
|---|---|---|---|
| No sampling | 0.0000 | 0.0010 | |
| Split sampling | 0.0000 | 0.0003 | 0.2147 |
| Bootstrap validation | - | - | 0.3718 |

The faulting model was successfully calibrated to reflect observed faulting for rigid pavements in the State of Michigan. The standard error and bias were reduced for all sampling techniques. The following are the limitations for the current faulting model local calibration:

a. A limited number of pavements sections were available for the local calibration of rigid pavements, and
b. The measured faulting values for the selected pavement sections were very low (less than 0.1 inches). Since, the most of rigid pavement (JPCP) in the State of Michigan are young (less than 10 years old) and are doweled at transverse joints. Low levels of faulting are expected.

The above limitations are mostly observed faulting data related and therefore can be rectified in the future calibrations of the model when sufficient faulting magnitudes and more pavement sections are available. However, the methodology of the faulting model local calibration is documented which can be adopted for future calibration efforts.

**Summary of Findings**

The local calibration of the faulting model entails changing all the calibration coefficients simultaneously. In order to accomplish this goal, the predicted faulting values need to be calculated outside the Pavement-ME software. Such an endeavor could be challenging, especially when appropriate models are not available to determine the recursive solution for faulting predictions. This paper has addressed the local calibration of the faulting model in the State of Michigan. The results of the paper show that resampling methods such as bootstrapping can assist in determining more robust estimates of the calibration coefficients, especially when the data are scarce. In order to get an adequate local calibration of the faulting model, the magnitude of observed faulting in the calibration data set should be of practical value since the prediction model can be used for a range of conditions under a given environment.

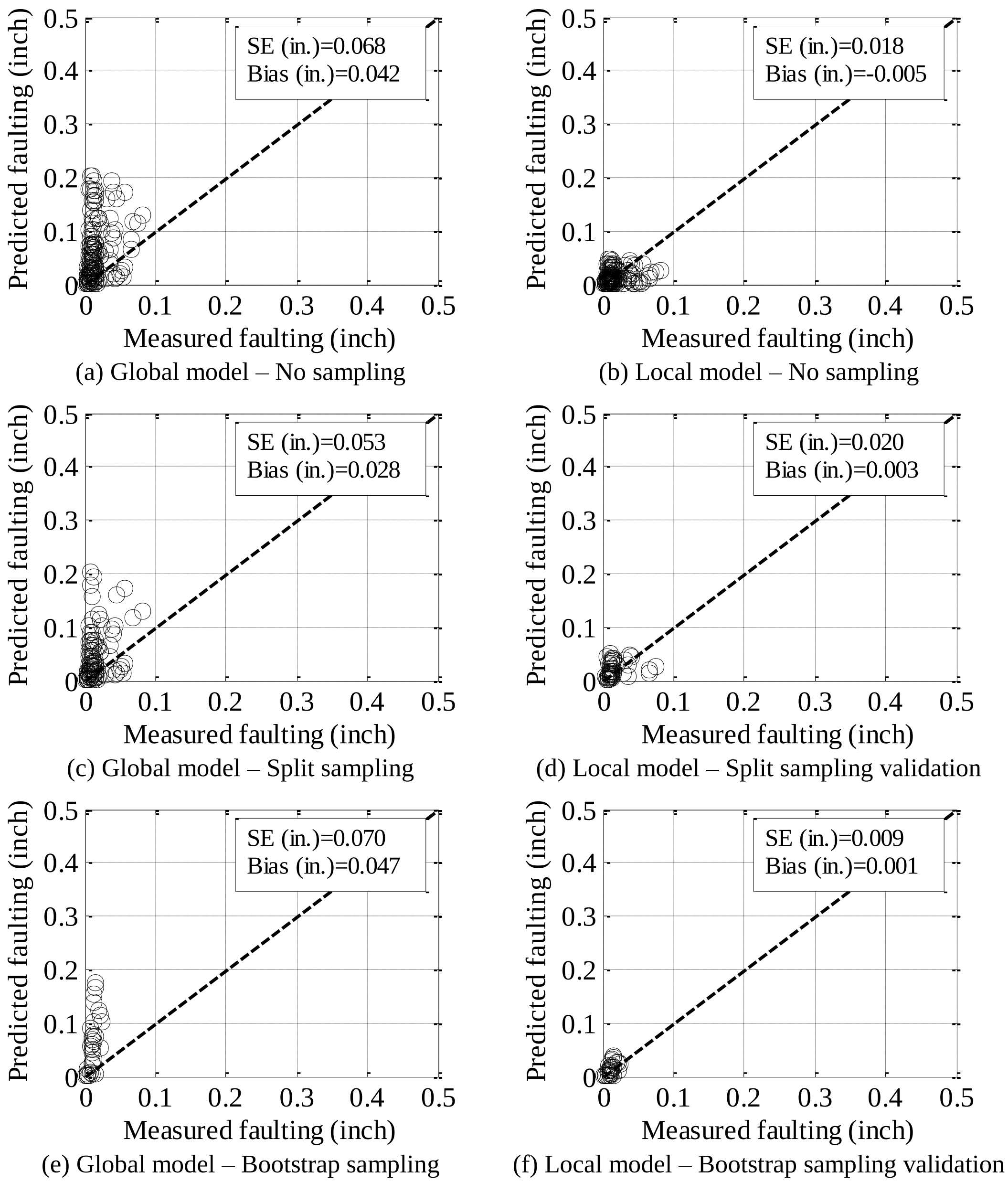


(a) Global model – No sampling

(b) Local model – No sampling

(c) Global model – Split sampling

(d) Local model – Split sampling validation

(e) Global model – Bootstrap sampling

(f) Local model – Bootstrap sampling validation

Figure 8 Measured versus predicted faulting before and after local calibration

## References


AASHTO (2008). "Mechanistic-Empirical Pavement Design Guide: A Manual of Practice: Interim Edition." American Association of State Highway and Transportation Officials.

Fick, S. B. (2010). "Evaluation of the AASHTO Empirical and Mechanistic-Empirical Pavement Design Procedures using the AASHO Road Test." Master of Science, University of Maryland, College Park.

Haider, S. W., Buch, N., Brink, W., Chatti, K., and Baladi, G. Y. (2014). "Preparation for Implementation of the Mechanistic-Empirical Pavement Design Guide in Michigan - Part 3: Local Calibration and Validation of the Pavement-ME Performance Models." Michigan Department of Transportation.

Mallela, J., Titus-Glover, L., Bhattacharya, B. B., Gotlif, A., and Darter, M. I. (2015). "Recalibration of the JPCP Cracking and Faulting Models in the AASHTO ME Design Procedure." *Transportation Research Board 94th Annual Meeting*(15-5222).

MathWorks (2015). "Global Optimization Toolbox User's Guide (R2015a)."

Pierce, L. M., and McGovern, G. (2014). "Implementation of the AASHTO Mechanistic-Empirical Pavement Design Guide and Software."

Sachs, S., Vandenbossche, J. M., and Snyder, M. B. "Calibration of the National Rigid Pavement Performance Models for the Pavement Mechanistic-Empirical Design Guide." *Proc., Transportation Research Board 94th Annual Meeting*.

Varma, S., Kutay, M., and Levenberg, E. (2013). "Viscoelastic Genetic Algorithm for Inverse Analysis of Asphalt Layer Properties from Falling Weight Deflections." *Transportation Research Record: Journal of the Transportation Research Board*(2369), 38-46.